Published in final edited form as:
Nat Neurosci. 2012 December ; 15(12): 1621–1623. doi:10.1038/nn.3263.

Impaired adult myelination in the prefrontal cortex of socially isolated mice

Jia Liu[1,4], **Karen Dietz**[1,4], **Jacqueline M DeLoyht**[2], **Xiomara Pedre**[1], **Dipti Kelkar**[1], **Jasbir Kaur**[1], **Vincent Vialou**[1], **Mary Kay Lobo**[1,3], **David M Dietz**[1,3], **Eric J Nestler**[1], **Jeffrey Dupree**[2], and **Patrizia Casaccia**[1]

[1]Department of Neuroscience and Friedman Brain Institute, Mount Sinai School of Medicine, New York, New York, USA.

[2]Department of Anatomy and Neurobiology, Virginia Commonwealth University, Richmond, Virginia, USA.

Abstract

Protracted social isolation of adult mice induced behavioral, transcriptional and ultrastructural changes in oligodendrocytes of the prefrontal cortex (PFC) and impaired adult myelination. Social re-integration was sufficient to normalize behavioral and transcriptional changes. Short periods of isolation affected chromatin and myelin, but did not induce behavioral changes. Thus, myelinating oligodendrocytes in the adult PFC respond to social interaction with chromatin changes, suggesting that myelination acts as a form of adult plasticity.

PFC is a brain region that is involved in complex emotional and cognitive behavior. Early social experiences in neonatal[1] or juvenile[2] animals result in defective developmental myelination, but it is unclear whether this form of plasticity persists in the adult brain. Given that neuroimaging studies in human subjects[3] support the concept of ongoing PFC myelination until the third decade of life, we asked whether depriving adult mice of social contact[4] would affect adult PFC myelination. After 8 weeks of social isolation[4], we did not detect any difference in locomotion between isolated mice and group-housed controls (traveled distance = 1,060 ± 58 cm in controls and 1,187 ± 57.6 cm in isolated, average ± s.e.m.) . However, the isolated mice spent significantly less time interacting with a conspecific mouse (68.65 ± 4.6 s, average ± s.e.m., $n = 21$) compared with group-housed peers (86.92 ± 4.3 s, average ± s.e.m., $n = 19$; $P = 0.006$), a sign of social withdrawal. Ultrastructural analysis revealed healthy myelinated axons in PFC, with intact nodal and paranodal structures (Supplementary Fig. 1a), and stable nodal lengths (Supplementary Fig. 1b). Transcript levels for neuronal-specific nodal and paranodal genes (that is, *Scn2a1*,

Correspondence should be addressed to P.C. (patrizia.casaccia@mssm.edu). .
[3]Present addresses: Department of Anatomy and Neurobiology, University of Maryland School of Medicine, Baltimore, Maryland, USA (M.K.L.), Department of Pharmacology and Toxicology, University of Buffalo School of Medicine, Buffalo, New York, USA (D.M.D.).
[4]These authors contributed equally to this work.

Note: Supplementary information is available in the online version of the paper.

AUTHOR CONTRIBUTIONS J.L. and K.D. performed the experiments, contributed to data acquisition and analysis, and wrote the paper. X.P., D.K., M.K.L. and J.K. assisted with data acquisition. D.M.D. and V.V. provided behavioral analysis. J.M.D. and J.D. contributed to the ultrastructural analysis. J.D. and E.J.N. contributed to data interpretation and wrote the paper. P.C. ideated and directed the project, analyzed the data and wrote the paper.

COMPETING FINANCIAL INTERESTS The authors declare no competing financial interests.

NFasc186 and *Cntnap1*) were stable (Supplementary Fig. 1c), whereas expression of oligodendrocyte-specific paranodal genes (that is, *NFasc155* and *Cntn2*) decreased in the isolated mice compared with control mice. On the basis of these findings and the stability of nodal proteins[5], we conclude that behavioral changes are not attributable to structural nodal changes. We then investigated myelination changes in mice deprived of social stimuli. Ultrastructural analysis revealed thinner myelin sheaths in PFC, but not in the corpus callosum or other areas associated with motivational aspects of social interaction (for example, nucleus accumbens), of isolated mice compared with controls (Fig. 1a). Quantification of myelin thickness relative to axonal diameter (that is, *g* ratio) revealed statistically significant differences between group-housed ($g = 0.810 \pm 0.01$, average ± s.e.m.) and socially isolated ($g = 0.876 \pm 0.01$) mice in PFC ($P < 0.005$; Fig. 1b). These differences in myelin thickness and *g* ratio were not detected in areas involved in locomotor behavior, such as the cerebellum (Fig. 1c,d).

Decreased myelin gene transcripts were also detected in regions that are functionally relevant to the control of social behavior, such as PFC (Fig. 2a), but not in corpus callosum or nucleus accumbens (Fig. 2b), of isolated mice and were paralleled by changes in proteins (Fig. 2c and Supplementary Fig. 2). These changes were not specific to males, as decreased myelin transcripts and proteins were also detected in isolated females (Supplementary Fig. 2). These transcriptional changes are unlikely to be attributable to cell death, as oligodendrocyte transcript levels remained stable (Supplementary Fig. 1d), the numbers of oligodendrocytes in the PFC of *Cnp-EGFP* transgenic mice (Fig. 2d) were similar in both isolated mice (48.38 ± 1 cells) and controls (50.95 ± 3 cells, average ± s.e.m., $n = 3$ per group) and we did not detect pyknotic nuclei, myelin debris or microglial activation. To explore whether hypomyelination was a result of delayed myelin formation, we analyzed nuclear chromatin condensation as an additional parameter associated with maturation of oligodendrocytes, as it is observed during development (Supplementary Fig. 3). Notably, in the isolated mice, the detection of axons with thinner myelin was associated with the presence of oligodendrocytes with immature nuclear chromatin (Fig. 2e) and with a lower proportion (Fig. 2f) of nuclear heterochromatin (56.7 ± 9.8% of heterochromatin in isolated and 66.8 ± 7% in controls, average ± s.e.m.). Histone deacetylation is required for oligodendrocyte differentiation and chromatin compaction, whereas high levels of histone acetylation are associated with impaired myelination and euchromatic nuclei[6–9]. The lower percentage of heterochromatin in PFC of isolated mice was consistent with the presence of euchromatic nuclei characterized by higher (1,996 ± 111 pixels per area in isolated and 1,681 ± 57 in controls) levels of histone acetylation (Fig. 2g) and lower levels of repressive (868.3 ± 23.75 pixels per area in isolated and 1,541 ± 45 in controls) histone methylation marks (Fig. 2h). These changes paralleled decreased transcripts for enzymes regulating histone acetylation (Fig. 2i) and repressive histone methylation (Fig. 2j). Together, these results suggest a working model of myelin plasticity in the adult brain that is in part mediated by changes in nuclear heterochromatin induced by prolonged social isolation and leads to impaired myelin formation.

We then asked whether a briefer period of social isolation (15 d) would be sufficient to induce similar behavioral, transcriptional and ultrastructural changes in adult mice. We did not detect decreased social interaction time (73.05 ± 4.3 s in isolated and 69.22 ± 4.2 s in controls) or changes in myelin gene transcripts (Fig. 3a) in PFC of mice after 2 weeks in isolation. However, ultrastructural analysis revealed slightly decreased myelin thickness (Fig. 3b) and modestly increased *g* ratio (Fig. 3c) compared with controls. The most notable change was decreased percentage of heterochromatin (Fig. 3d,e) and the presence of cytoplasmic islands (Supplementary Fig. 4a) and redundant profiles (Supplementary Fig. 4b), characteristic of immature myelin. Thus, 2 weeks of social isolation in adult mice induced significant ($P < 0.0001$) changes in heterochromatin that likely preceded changes in

social behavior. We then asked whether juvenile (3 week old) mice were more susceptible to brief social isolation periods, as a result of lower chromatin condensation at younger ages. After 2 weeks of isolation, we detected differences in myelin thickness (Fig. 3f), higher *g* ratios (Fig. 3g) and a lower percentage of heterochromatin in juvenile mice (Fig. 3h,i), which is consistent with recent results in mice isolated immediately after weaning[2].

Together, our data support a model of adult myelin plasticity that involves chromatin condensation and oligodendrocyte differentiation in response to external stimuli, possibly resulting in epigenetic modulation of gene expression. Plasticity, however, implies reversibility. For this reason we performed a social-reintegration experiment and group-housed adult mice for 4 weeks that were previously kept in isolation for 8 weeks (Supplementary Fig. 5). Consistent with adult myelin plasticity model, social re-integration allowed a return of myelin transcripts to control levels and normalized social interaction behavior (Supplementary Fig. 5). Thus, we suggest that myelination in PFC of adults is modified by social experience and that this change is manifested as social withdrawal.

The PFC integrates external stimuli and controls several domains of complex behavior[4], and myelin changes in this area have been reported in a wide range of psychiatric illnesses, including autism, anxiety, schizophrenia and depression[10]. Models of juvenile social isolation result in myelination changes that mimic conditions related to neurodevelopmental disorders and have recently been shown to resemble the phenotype of mice with decreased ErbB3 signaling[2]. These myelination changes have been reported to be stable and partially explain the long-term consequences of early childhood experience on the development of psychiatric disorders in adulthood. Our study addresses a very different question by asking whether the ongoing myelination occurring in adult PFC renders this region more prone to using myelination as a form of plasticity to adapt brain function to environmental stimuli. This plasticity has been proposed as a way of adapting myelin thickness to axonal firing rate[11]. We found that prolonged social deprivation decreased myelin thickness in PFC of adult mice and was associated with defective heterochromatin formation in oligodendrocytes. Our data suggest a model in which a socially stimulating environment and associated PFC neuronal activity signal chromatin changes to oligodendrocytes via neuronally derived signals (neuregulins or unknown factors). This would in turn initiate a program of differentiation, possibly involving epigenetic regulation of gene expression and culminating with axonal myelination. A corollary of such a model would predict that new myelin formation is stalled by a lack of social stimuli. Post-translational modifications of nuclear histones and chromatin condensation are crucial for developmental myelination[7,9] and successful repair from demyelination[6]. We show here that these events are also affected by inadequate social stimulation. Consistent with the concept of adult plasticity, and at variance with reports on juvenile isolation, the transcriptional and behavioral changes that we observed were reversed by social re-integration.

White matter abnormalities occur in psychiatric conditions characterized by social withdrawal[12–14] in response to stress[15]. Conversely, demyelinating disorders characterized by myelin loss show co-morbidity with depression[16]. The translational application of our findings supports the importance of maintaining a healthy lifestyle and socially stimulating environment, especially in pathologies characterized by lost or damaged myelin.

ONLINE METHODS

Social isolation

All experimental C57Bl/6J male mice were obtained from the Jackson Laboratory and maintained in a temperature- and humidity-controlled facility on a 12-h light-dark cycle with food and water *ad libitum*. The *Cnp-EGFP* mice were a kind gift from V. Gallo (Children's

National Medical Center). All procedures were carried out in accordance with the Institutional Animal Care and Use Committee guidelines of the Mount Sinai School of Medicine. Mice were either singly housed or group housed (five mice per cage) for a duration of 2–8 weeks. During the regroup experiment, three mice were housed per cage at the end of isolation period for 4 weeks.

Social interaction test

The behavioral assessment used was adapted from a previous description[17]. A video-tracking system was used to score approach-avoidance behaviors toward an unfamiliar social target. The arena was a white plastic open field (42 × 42 cm) maintained in complete darkness. Video recordings were made using a camera equipped with infrared filter and lights. Each experimental mouse was introduced into the open field and its trajectory was tracked for two consecutive sessions of 2.5 min, a test duration chosen for its optimal sensitivity to throughput ratio. During the first session (no target), the open field contained an empty wire mesh cage (10 × 6.5 cm) located at one end of the field. During the second session (target), the conditions were identical except that a social target animal (an unfamiliar C57Bl/6 male mouse) had been introduced into the cage. Between the two sessions, the experimental mouse was removed from the arena and placed back into its home cage for approximately 1 min. The video-tracking data from both the no target and target conditions were used to determine the time spent by the experimental mouse in the interaction zone (an 8-cm-wide corridor surrounding the cage) and the corners of the open field opposite to the location of the cage. A two-tailed Student's *t* test was performed to assess statistical differences between control (group housed) and isolated conditions at a significance level of $P < 0.05$.

RNA tissue extraction and analysis

Tissue punches were taken from the medial PFC, nucleus accumbens and corpus callosum and flash frozen for subsequent processing. RNA was extracted using Trizol (Invitrogen, #15596-018) and purified with the RNeasy Micro kit (Qiagen, #74004) following the manufacturer's protocol. RNA was reverse transcribed with qScript cDNA Supermix (Quanta, #95048) and qRT-PCR was performed using Perfecta Sybr Fast Mix Rox 1250 (Quanta, #101414-278) at the Mount Sinai Shared Resource Facility (primers listed in Supplementary table 1). Each transcript value was calculated as the average of triplicate samples from several mice per experimental condition (typically 4–6). After normalization to *Gapdh*, the average values for each transcript was calculated based on the values obtained in all the samples included for each experimental condition. Two tailed Student's *t* tests were performed to assess statistical differences between the average values in each condition, and a FDR correction was applied for multiple testing in gene groups (that is, myelin genes, nodal genes, acetyltransferase/deacetyltransferase genes and methyltransferase genes), with a significance threshold of 0.05. Two-tailed Student's *t* tests were performed to assess statistical differences between the average values in each condition, and a FDR correction was applied for multiple testing in gene groups (myelin genes, nodal genes, acetyltransferase/deacetyltransferase genes and methyltransferase genes), with a significance threshold of 0.05.

Electron microscopy

Mice were processed for standard electron microscopic analysis as previously described with slight modifications[18,19]. Briefly, following transcardial perfusion of appropriately aged mice, brains were harvested and vibratome sectioned to locate the regions of interest (PFC, nucleus accumbens and anterior commissure). Following post-fixation, dehydration and resin infiltration, the sections were sandwiched between Rinzle plastic microscope slides (EMS Sciences). After polymerization, the sections were mounted on PolyBed studs

for thick (1 μm) and thin (90 nm) sectioning. Thick sections were stained with toluidine blue and analyzed with a Nikon ECLIPSE E800M equipped with a Diagnostic Instruments Spot RT CCD camera. Uranyl acetate and lead citrate stained thin sections were imaged using a JEOL JEM 1230 transmission electron microscope equipped with Gatan Ultrascan 4000 digital camera. The extent of heterochromatin was determined using electron micrographs (5,000×) of individual oligodendrocyte lineage cells. Oligodendroglial cells were identified by the presence of microtubules combined with the absence of intermediate filaments and glycogen granules. Using ImageJ (US National Institutes of Health)[20], the nucleus of each cell was isolated using the 'clear outside' function and total nuclear area was calculated. Heterochromatin, qualitatively defined as a gray scale density of 100 or greater on a 256 gray scale, was selected using the threshold tool and reported as percentage of total nuclear area. Extent of myelination was quantitatively compared by determining *g* ratios, which were calculated by dividing the diameter of the axon by the diameter of the entire myelinated fiber as previously described (187). For this analysis, ImageJ was used to measure both axon caliber and myelin fiber diameter for a minimum of 100 myelinated axons per animal. Two-tailed Student's *t* tests were performed to assess statistical differences between isolated and grouped mice.

Immunohistochemistry

Experimental animals were anesthetized and then perfused with 4% (wt/vol) paraformaldehyde in 0.1 M phosphate buffer. Whole brains were removed from the skulls, post-fixed, cryopreserved in 30% (wt/vol) sucrose, embedded in OCT and sectioned coronally (14 μm). Frozen sections were first permeabilized with blocking buffer (0.1 M phosphate buffer, 10% (vol/vol) normal goat serum (Vector Laboratories) and 0.5% (vol/vol) Triton X-100). Incubation with primary antibodies was performed overnight at 4 °C. Prior to staining with acetyl H3 (Upstate 06-599, 1:500) or H3K9me3 (Abcam ab8898, 1:100) and CC1 (Calbiochem OP80, 1:50), antigen retrieval was performed in10 mM citrate buffer (pH 6.0) for 2 h at 65 °C. Staining with primary antibodies to MBP (Covance SMI99, 1:500) and NG2 (Chemicon AB5320, 1:200) occurred after antigen retrieval with methanol at −20 °C for 10 min. A 1-h incubation with secondary fluorescent antibodies (Alexa Fluor 488 or 546) was performed the following day with counterstaining for DAPI (1:1,000, Molecular Probes). Stained sections were visualized using confocal microscopy (LSM710 Meta confocal laser scanning microscope, Carl Zeiss Micro-Imaging). The pixel intensity of H3ac and H3K9me3 was quantified using ImageJ. Approximately 20–40 $CC1^+$ cells close to the midline of PFC were counted in each animal. Two-tailed Student's *t* tests were performed to assess statistical differences between control and experimental conditions after combing the total number of cells in each group.

Western blot

Protein were extracted using lysis buffer containing 50 mM HEPES (pH 7.4), 150 mM NaCl, 10% (vol/vol) glycerol, 1 mM EDTA (pH 8.0), 1% (vol/vol) NP-40, 1 mM DTT, 1 mM PMSF, and protease and phosphatase inhibitors. Western blot analysis was performed using appropriate dilution of primary antibodies (antibody to Mbp, Covance SMI99, 1:1,000) and secondary antibodies (horseradish peroxidase–conjugated antibody to mouse, 1:10,000, Vector Laboratories). The immunoreactive bands were detected by ECL Plus Western Blotting Detection System (GE Health Care Life Sciences). Equal protein loading was guaranteed by probing the blots with antibody to beta-actin (Sigma A5316, 1:5,000). Densitometry of the western blot protein bands was analyzed using ImageJ. Statistical analysis was performed using two-tailed Student's *t* tests.

Supplementary Material

Refer to Web version on PubMed Central for supplementary material.

Acknowledgments

We thank A. Sharp, P. Garg and J. Huynh for help with statistical analysis and multiple correction tests. This work was funded by the US National Institutes of Health (R37-NS42925-10 to P.C. and P50-MH96890 to E.J.N.), a Center core grant to the Virginia Commonwealth University Microscopy Facility (5P30NS047463) and the National Multiple Sclerosis Society (FG1874-A-1 to J.L.).

References

1. Kikusui T, Kiyokawa Y, Mori Y. Brain Res. 2007; 1133:115–122. [PubMed: 17184748]
2. Makinodan M, Rosen KM, Ito S, Corfas G. Science. 2012; 337:1357–1360. [PubMed: 22984073]
3. Fuster JM. J. Neurocytol. 2002; 31:373–385. [PubMed: 12815254]
4. Wallace DL, et al. Nat. Neurosci. 2009; 12:200–209. [PubMed: 19151710]
5. Pillai AM, et al. J. Neurosci. Res. 2009; 87:1773–1793. [PubMed: 19185024]
6. Shen S, et al. Nat. Neurosci. 2008; 11:1024–1034. [PubMed: 19160500]
7. Shen S, Li J, Casaccia-Bonnefil P. J. Cell Biol. 2005; 169:577–589. [PubMed: 15897262]
8. Ye F, et al. Nat. Neurosci. 2009; 12:829–838. [PubMed: 19503085]
9. He Y, et al. Neuron. 2007; 55:217–230. [PubMed: 17640524]
10. Regenold WT, et al. Bipolar Disord. 2006; 8:188–195. [PubMed: 16542190]
11. Fields RD. Trends Neurosci. 2008; 31:361–370. [PubMed: 18538868]
12. Sokolov BP. Int. J. Neuropsychopharmacol. 2007; 10:547–555. [PubMed: 17291372]
13. Sexton CE, Mackay CE, Ebmeier KP. Biol. Psychiatry. 2009; 66:814–823. [PubMed: 19615671]
14. Rajkowska G, et al. Biol. Psychiatry. 1999; 45:1085–1098. [PubMed: 10331101]
15. Chari DM, et al. J. Neurosci. Res. 2006; 83:594–605. [PubMed: 16429447]
16. Arnett PA, Barwick FH, Beeney JE. J. Int. Neuropsychol. Soc. 2008; 14:691–724. [PubMed: 18764967]
17. Berton O, et al. Science. 2006; 311:864–868. [PubMed: 16469931]
18. Marcus J, et al. Glia. 2006; 53:372–381. [PubMed: 16288467]
19. Shroff SM, et al. J. Neurosci. Res. 2009; 87:3403–3414. [PubMed: 19224580]
20. Abramoff MD, Magalhães PJ, Ram SJ. Biophotonics Int. 2004; 11:36–42.

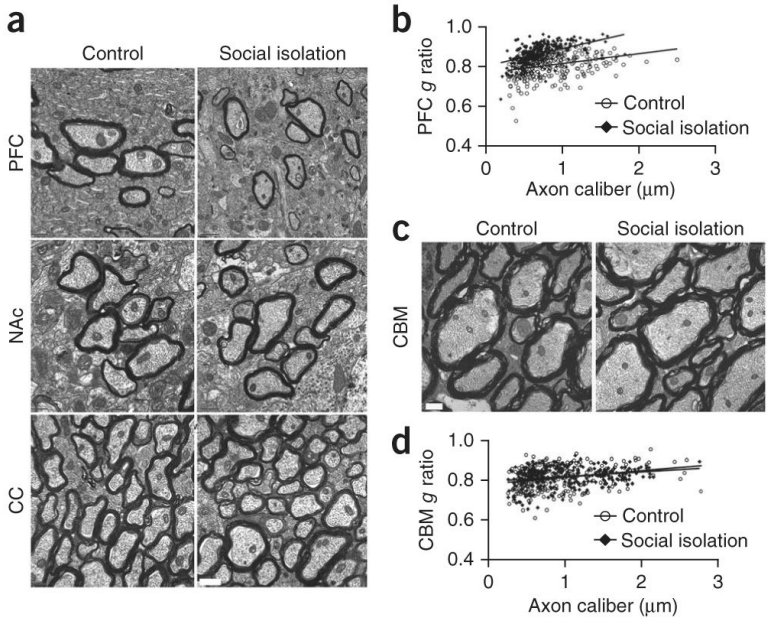

Figure 1.

Prolonged social isolation of adult mice induces hypomyelination in PFC. (**a**) Electron micrographs of axons in the PFC, nucleus accumbens (NAc) and corpus callosum (CC) from control and isolated mice. Scale bar, 0.5 μm. (**b**) Scatter plot of *g* ratio values in the PFC in group-housed controls ($n = 315$ axons) and isolated ($n = 321$ axons) mice. (**c**) Electron micrograph of axons in the cerebellum (CBM) from isolated and control mice. Scale bar, 0.5 μm. (**d**) Scatter plot showing *g* ratio values in the CBM of control ($n = 239$) and isolated ($n = 290$ axons) mice.

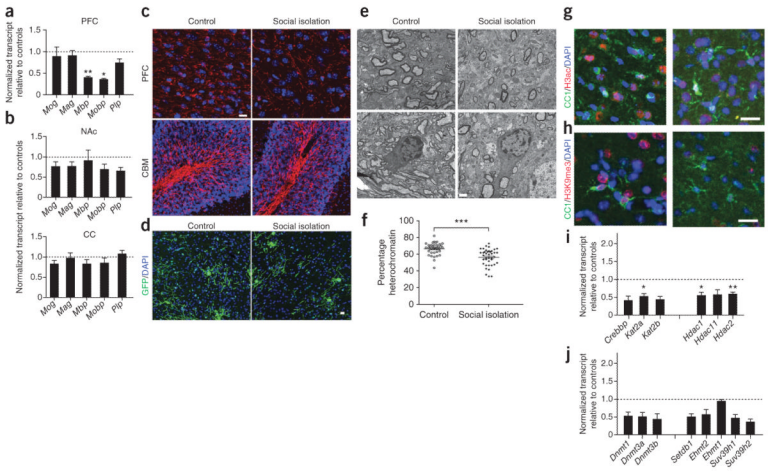

Figure 2.

Prolonged social isolation of adult mice decreases myelin gene products and heterochromatin formation. (**a,b**) Quantitative real-time-PCR (qRT-PCR) of myelin gene transcripts in nucleus accumbens, corpus callosum and PFC. Bar graphs indicate average values in six isolated mice after *Gapdh* normalization relative to average control levels (dashed line) (*false discovery rate (FDR) < 0.05, **FDR < 0.01). (**c**) Confocal images of Mbp^+ (red) myelinated fibers in PFC and cerebellum. DAPI (blue) was used as nuclear counterstain. Scale bar, 10 μm. (**d**) Confocal images of oligodendrocytes in the PFC of isolated and group-housed *Cnp-EGFP* mice. (**e**) Electron micrographs of PFC showing myelinated axon (top) and relative appearance of oligodendrocyte nuclei (bottom) in isolated and control mice. Scale bar, 1 μm. (**f**) Scatter plot of the percentage nuclear heterochromatin in PFC oligodendrocytes from control ($n = 36$ nuclei) and isolated ($n = 40$ nuclei) mice (***$P < 0.001$). (**g,h**) Confocal images of $CC1^+$ oligodendrocytes (green) colabeled with antibodies for acetylated histone marks (H3ac, red, **g**) or repressive methylation marks (H3K9me3, red, **h**). Scale bars, 10 μm. (**i,j**) qRT-PCR analysis of transcripts of enzymes regulating histone acetylation (**i**) and repressive DNA and histone methylation (**j**). Data are presented as in **a** and **b**. Error bars, s.e.m.

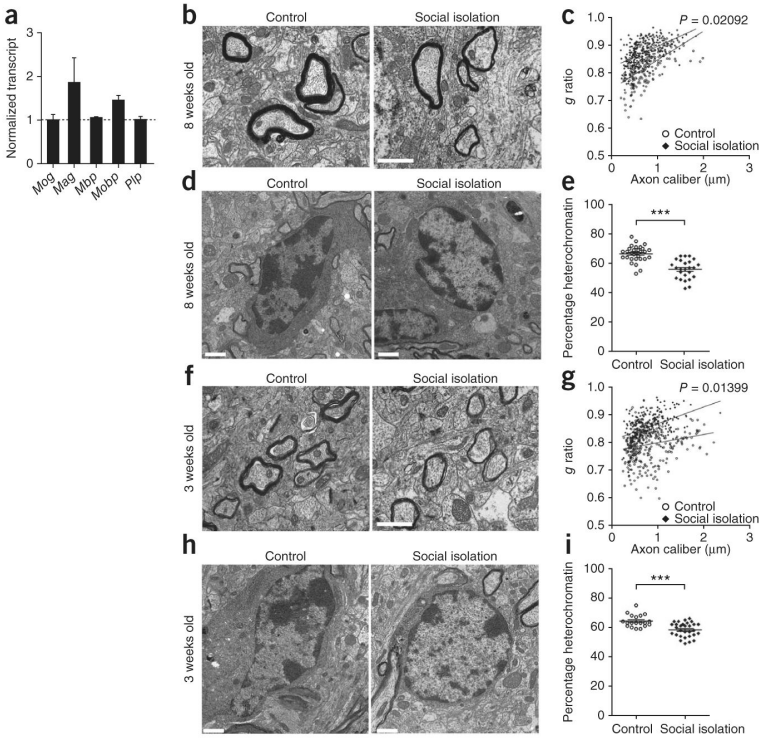

Figure 3.

Short-term isolation is sufficient to induce chromatin changes and reduce myelin thickness in both adult and juvenile mice. (**a**) qRT-PCR of myelin transcripts in the PFC of adult (8 week old) mice after 2 weeks of social isolation. Bar graphs indicate average values for isolated mice after *Gapdh* normalization and are presented as relative values to average control levels (dashed line). (**b,f**) Electron micrographs of axons in PFC of adult (**b**) and juvenile (**f**) mice after 2 weeks of social isolation. Scale bars, 1 μm. (**c**) Scatter plot of *g* ratio values in adult PFC of isolated ($n = 279$ axons) and control ($n = 200$ axons) mice. (**d,h**) Electron micrographs of oligodendrocyte nuclei in PFC of adult (**d**) and juvenile (**h**) mice in control housing or isolated for 2 weeks. Scale bars, 1 μm. (**e,i**) Scatter plot of the percentage of nuclear heterochromatin in PFC oligodendrocytes in adult (**e**) isolated ($n = 40$ nuclei) and control ($n = 36$ nuclei) mice and juvenile (**i**) isolated ($n = 30$ nuclei) and control ($n = 19$ nuclei) mice. (**g**) Scatter plot of *g* ratio values in juvenile PFC of isolated ($n = 248$ axons) and control ($n = 333$ axons) mice. ***$P < 0.001$. Error bars, s.e.m.